Earthquake Engineering, Tenth World Conference © 1992 Balkema, Rotterdam. ISBN 90 5410 060 5

Risk spectrum taking into account fault rupture mechanisms

J. Kiyono & T. Sato
Disaster Prevention Research Institute, Kyoto University, Japan

ABSTRACT: Historical earthquake records provide information for the past few hundred years, whereas active fault data is based on the seismic activity over millions of years. Combined use of both types of data is the most effective approach for estimating seismic risk. Using Bayes' theorem, we have evaluated the seismic hazard in the Kinki district, Japan from a combination of historical earthquake records and active fault data.

The risk spectrum at bed rock level for the return period is determined from the attenuation equation of the response spectrum. This attenuation equation is derived by simulating the maximum response acceleration taking into account fault rupture mechanisms.

1 INTRODUCTION

When designing civil structures it is necessary to have realistic and reliable seismic hazard assessments. Many risk analyses have been made with various probabilistic models (Cornell 1968, Kiureghian 1977). Most hazard prediction methods are in the form of the exceedance of a seismic intensity during a specified time period. Engineering risk analyses in Japan mainly are based on historical earthquake records (Katayama 1982). Methods that combine the use of these records and active fault data are rare (Kameda 1985). Kameda and his associates defined the joint earthquake occurrence rate by using a value for the occurrence rate based on historical earthquake records and active fault data.

Earthquake ground motion depends on such factors as the source mechanism and geological features of the path and site. These factors are so complex that the only possible approach is to estimate input earthquake motion at the base rock level. We here report the calculations needed to obtain the uniform risk spectrum at that level. The methodology involves describing the seismic source and the attenuation of the amplitude of seismic motion.

We estimated the seismic hazard from the combined available historical earthquake information and active fault data, incorporating the Baisian approach. The seismic hazard for the active fault data then was estimated from the fault rupture model (Sato 1986). Seismic risk spectra for the city of Osaka, Japan were obtained from the source model.

2 EARTHQUAKE OCCURRENCE RATE AND SEISMIC RISK ANALYSIS

2.1 Historical earthquake records

The historical earthquake information for the area within a 300 km radius of Osaka that was used in this analysis is given in Figure 1. Information was taken from the catalogue of disaster earthquakes (Usami 1975, Utsu 1979). The cross, triangle, circle and square in the figure respectively correspond to ranges of magnitude of 5 - 6, 6 - 7, 7 - 8 and 8 -.

Suppose that n_h historical data are obtained over T years in the region in which the radius from the site is 300 km. For the earthquake occurrence rate, ν_h, the acceleration, α, exceeds the value, α^*, at the site such that

$$\nu_h = P(\alpha<\alpha^*)\ \nu'_h \qquad (1)$$

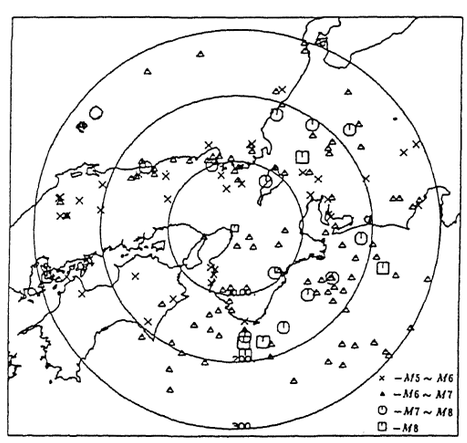

Figure 1. Historical earthquake data for the Kinki district, Japan.

in which $P(\alpha<\alpha^*)$ is the probability of the acceleration α exceeding α^* at an arbitrary site in that region, and ν'_h is the average rate of earthquake occurrence in the region. The probability, $P(\alpha<\alpha^*)$, is found from the attenuation equation at the base rock level (Ejiri 1990A), for which the shear wave velocity is about 3 km because, in our procedure, the peak acceleration at base rock level is calculated first, then the amplification factors of the site are considered.

Assuming that earthquake occurrence obeys the Poisson process with an average occurrence rate of ν_h, the probability of having n events in period T can be determined. As the probability that no special events that exceed α^* occur in a year is $\exp(-\nu_h)$, the annual exceedance, F_{ph}, and the average return period, T_{rh}, are

$$F_{ph} = 1 - \exp(-\nu_h) \tag{2}$$

$$T_{rh} = \frac{1}{F_{ph}} \tag{3}$$

The amplification factor of the site is multiplied for the input wave at the base rock level on the basis of the existing geological conditions (Midorikawa 1985). A hazard map for the Kinki district established by the above procedure is shown in Figure 2. The return period is 100 years. Peak accelerations of more than 100 gal are expected in the south part of the Kii Peninsula, in the area from Osaka Bay to Lake Biwa, and in the vicinity of Ise Bay.

2.2 Active fault data

For the digitization of the fault data, the active fault is idealized as a straight line. The total number of faults in this data set are 887 (Ejiri 1990B). The faults in the Kinki district are shown in Figure 3. The faulting mechanism is the maximum moment model (Wesnousky 1983) which assumes that the earthquake occurrence rate, ν_i, on a fault, *i*, is equal to the ratio of the geologically determined rate of moment release ($\dot{M}_0$) to the seismic moment of the maximum expected earthquake (M_0^{max}) on a fault;

$$\nu_i = \frac{\dot{M}_0}{M_0^{max}} \tag{4}$$

An earthquake occurrence rate is supposed for which the acceleration, α, exceeds the value, α^*, at a specified site. The smallest magnitude, m_0, is 5.0 and the radius of the affected region is assumed to be 300 km within which the occurrence of earthquakes would affect the site in terms of engineering concerns. This conditional earthquake occurrence rate, $\hat{\nu}_i$, on a fault, ***i***, in the region is

$$\hat{\nu}_i = P(\alpha>\alpha^*|E_i)\,\nu_i \tag{5}$$

$$\nu_f = \sum_{i=1}^{n_f} \hat{\nu}_i \tag{6}$$

in which $P(\alpha<\alpha^* \mid E_i)$ is the conditional probability of the acceleration α exceeding α^* at the site when an event of $m>m_0$ occurs on that fault and ν_f is the average occurrence rate for the region. The probability $P(\alpha<\alpha^* \mid E_i)$ is derived from the attenuation equation. Because the probability that no special events exceeding α^* occur in a year is $\exp(-\nu_h)$, the annual probabil-

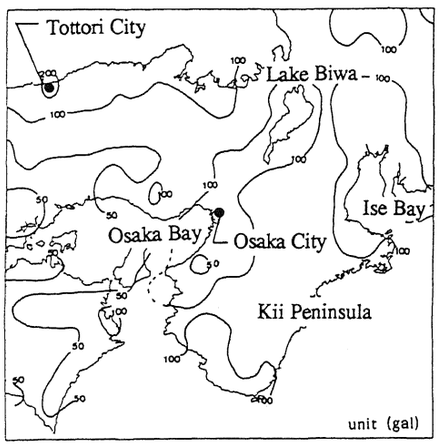

Figure 2. Seismic risk map of the Kinki district for the return period of 100 years calculated from historical earthquake data.

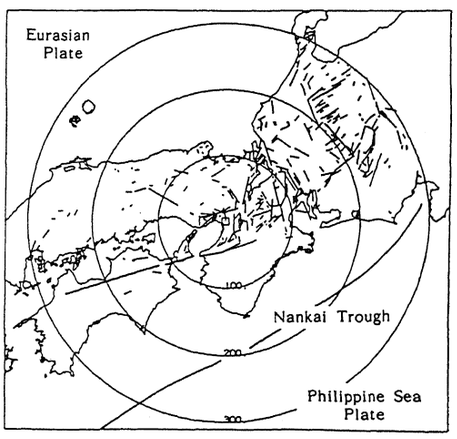

Figure 3. Active faults in the Kinki district.

ity of exceedance, F_{pf}, and the average return period, T_{rf}, are obtained from equations (2) and (3).

A risk map of the Kinki district for a return period of 100 years is shown in Figure 4. The southern part of the district is considered at risk because of the major fault that runs along the Pacific rim and the large interplate earthquakes that occur periodically in the region. Severe earthquakes, notably the 1854 Ansei Nankai Earthquake and the 1946 Nankai Earthquake, have occurred in the Nankai Trough, the interface between the Eurasian and Philippine Plates. We here deal only with intraplate earthquakes and mappable Quaternary faults, which is why the southern part of the Kii Peninsula is not shown as having a very high intensity level. The expected accelerations in places such as the Osaka Bay area and the vicinities of Lake Biwa and Ise Bay exceed 300 gal. This is because in these areas geological deposits have large amplification factors; moreover, the areas are adjacent to the group of intraplate faults.

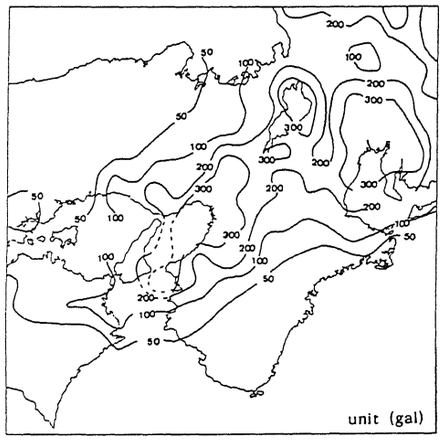

Figure 4. Seismic risk map of the Kinki district for the return period of 100 years calculated from active fault data.

2.3 Combination of earthquake occurrence rates

In the preceding sections, the annual earthquake occurrence rates for which the acceleration, α, exceeds the value, α^*, were calculated as ν_i for historical data and as the logarithmic normal distribution for active fault data. We here use Bayes' theorem to combine the active fault data and the information from historical earthquake records.

We assume that the prior distribution is described by the probability density function of the earthquake occurrence rate because active fault data obey a logarithmic normal distribution (μ, σ^2).

We obtained the average occurrence rate of earthquakes, ν_k, in the region from historical earthquake records. This means that earthquakes occur ν_k times per year; equivalent to a single earthquake occurring during $1/\nu_k$ year. Because the event-generating process is assumed to be a Poisson process, the likelihood function for ν is given by

$$L(\nu) = \frac{\nu}{\nu_h} \exp\left(-\frac{\nu}{\nu_h}\right) \tag{7}$$

Combining the prior distribution and the likelihood function by means of Bayes theorem, the posterior distribution, $f''(\nu)$, is given by

$$f''(\nu) = k\, L(\nu)\, f'(\nu) \tag{8}$$

After combining the historical earthquake and active fault data, the average occurrence rate of earthquakes is given by

$$\hat{\nu} = \int_0^\infty \nu f''(\nu) d\nu \tag{9}$$

An example of the combination according to Bayes' theorem is shown in Figure 5 for Osaka City. The prior distribution, $f'(x)$, obeys the logarithmic normal distribution, its mean value, ν, and variance, σ^2, being 2.0×10^{-3} and 3.6×10^{-6}. The square symbol in the figure is the posterior distribution, and the mean rate of occurrence is 2.6×10^{-3}.

The calculated hazard curves obtained from

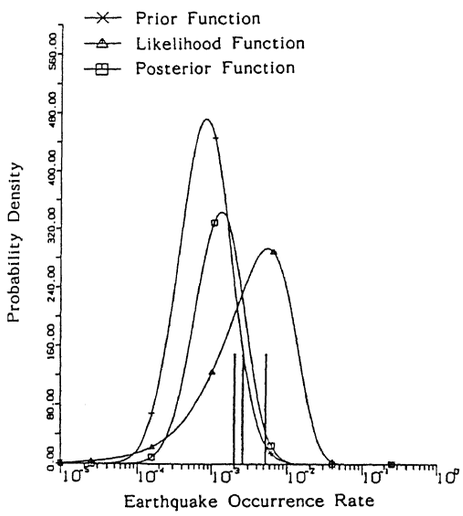

Figure 5. Prior distribution, likelihood function and posterior distribution.

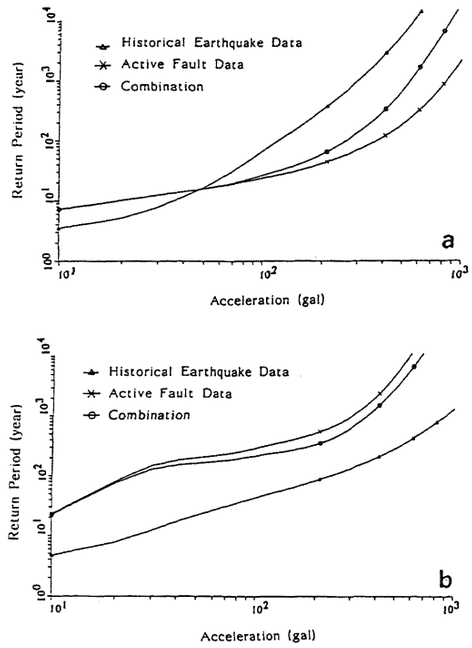

Figure 6. Comparison of hazard curves. (a) Osaka, (b) Tottori.

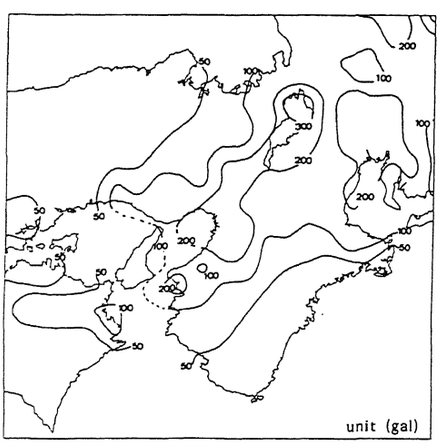

Figure 7. Seismic risk map of the Kinki district for the return period of 100 years calculated from combined historical earthquake information and active fault data.

historical earthquake records, actual fault data, and the combined data for Osaka City (34.7°N, 135.5°E) and Tottori City (35.6°N, 134.2°E) are shown in Figure 6 (a), (b). The abscissa shows the expected horizontal peak acceleration and the ordinate the return period. The peak accelerations for a return period of 100 years are expected to be 225 gal for Osaka and 25 gal for Tottori. The hazard map for the Kinki and Chugoku districts is shown in Figure 7. In this analysis, we assume that the prior distribution is logarithmic and normal, also that its deviation is very small. If the distributions of v that are based on historical and active fault information separate mutually, the distribution of v after combining both data sets approaches the prior distribution for the active fault data. The expected acceleration in the Chugoku district, as at Tottori, is small because of the lack of active fault data. Because the moment release rate for this area is very low, and the hazard curve can be estimated only from historical information this curve may contain many errors. Therefore our results, which are influenced by active fault data, are reasonable for the Chugoku district.

3 RISK SPECTRUM AT THE BASE ROCK LEVEL

We here show the theoretical simulation of the response spectrum at the base rock level (v_s=3km) and the attenuation equation of the maximum response acceleration for each natural period of that spectrum. A seismic risk analysis was made according to this attenuation law, and the risk spectrum for Osaka City calculated.

A large event is synthesized by superposing a number of small events. The motion of the large event, improved to take into account the high frequency component (Irikura 1983), is

$$g_L(t) = \sum_{i=1}^{N_L}\sum_{j=1}^{N_W} g_S(t-t_{ij}) + \sum_{i=1}^{N_L}\sum_{j=1}^{N_W}\sum_{k=1}^{(N_D-1)N'} \frac{1}{N'} g_S(t-t_{ijk}) \quad (10)$$

in which t_{lm} and t_{lmn} are the time delays caused by the superposition of the small events, and N_L, N_W, N_D the respective numbers of superpositions for length, width and dislocation.

Using the Fourier transform of equation (10), $G_L(f)$, and multiplying by the conjugate of $G_L(f)$ gives the power spectrum of the large event, $P_i(f)$. The path effect is taken into account by averaging the various reported Q-values. If we know the power spectrum of the earthquake motion at the bed rock level for a given M_i and Δ_i, the response power spectrum is obtained by multiplying the power spectrum by the response function, $H_{jk}(f \mid T_j, h_k)$, for a single degree-of-freedom system for which the natural period and damping constant are T_j and h_k.

$$R_{ijk}(\omega) = P_i(\omega)\, H_{jk}(\omega)\, H^*_{ij}(\omega) \quad (11)$$

Once the power spectrum of the large event is given, the expected maximum response acceleration can be estimated.

The approximate value of the maximum response acceleration is

$$S(T_j,h_k) = p\sqrt{\lambda_0} \qquad (12)$$

in which p is the peak coefficient and a function of m-th order spectrum moment (m=0,1,2). The magnitude, M_i, and the epicentral distance, Δ_i, are generated randomly in the ranges of $5.0<M_i<8.0$ and $0<\Delta_i<500$ km. The maximum response acceleration is computed for the magnitude and epicentral distance pair by varying T_j (0.1, 0.2, 0.5, 0.8, 1.0, 2.0, 5.0 sec) and h_k (0.02, 0.05, 0.10). The regression equation is written

$$\log \bar{S}_A(T_j,h_k) = c_1 + c_2M - c_3\log(\Delta+30) \qquad (13)$$

The obtained regression coefficients for seven natural periods are shown in Table 1. The damping constant is 5%.

Table 1. Regression coefficients for several natural periods (damping const.: 5%).

C \ T	0.10	0.20	0.50	0.80	1.00	2.00	5.00
c_1	6.16	5.41	4.01	3.34	3.08	2.59	1.28
c_2	0.24	0.25	0.30	0.37	0.37	0.38	0.48
c_3	3.06	2.76	2.32	2.24	2.17	2.05	1.95

The attenuation curve of maximum response acceleration for each natural period is shown in Figure 8. Taking into account the variance, S_{S_A}, of the attenuation equation, the average occurrence rate, v, in equation (9), which expresses the rate in which the response acceleration, S_A, exceeds the value for a natural period, S^*_A, is obtained by the procedure described in section 2. Assuming that the occurrence of earthquakes obeys the Poisson process with an average occurrence rate, v, obtained by combining separate occurrence rates based on the historical earthquake information and active fault data, the return period for the objective site at the base rock level can be calculated. Three hazard curves for T=0.8 sec and h=5% obtained for Osaka City are shown in Figure 9. These are based on the combined occurrence rates for seven natural periods (Figure 10). The risk spectrum based on these hazard curves is shown in Figure 11. The return period is 100 years. A comparison of this spectrum with the risk spectrum proposed by Furuta et al.(1990) that was calculated from the attenuation equation at the engineering base rock level (Sugito 1984) shows that the developed risk spectrum is smaller, especially in the low frequency range, because Sugito defines base rock level as the layer at which the S-wave velocity is 700-800 m/sec. If we can determine the amplification characteristics present between the base rock (v_s=3km) and upper layers, we can easily approximate the risk spectrum at any layer.

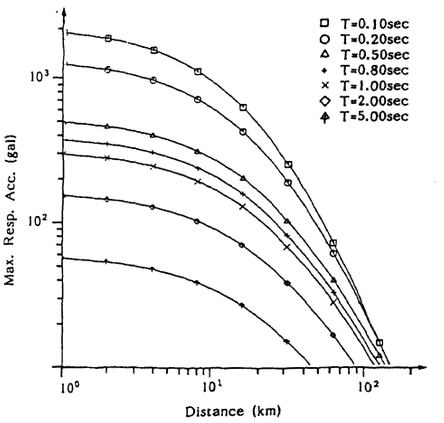

Figure 8. Attenuation curves of the maximum response acceleration for various natural periods.

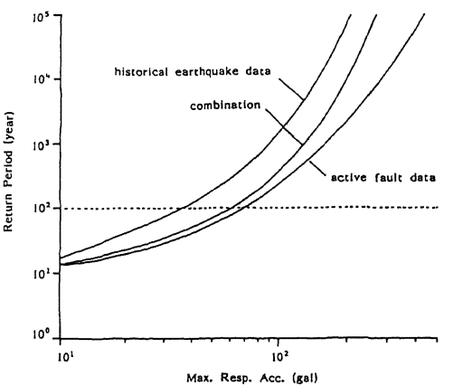

Figure 9. Three hazard curves for T=0.8 sec and h=5% for Osaka City.

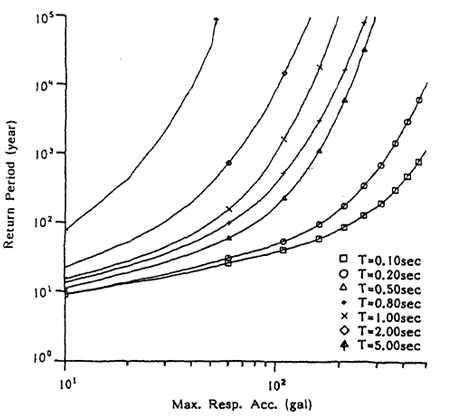

Figure 10. Hazard curves based on the combined occurrence rate for various natural periods.

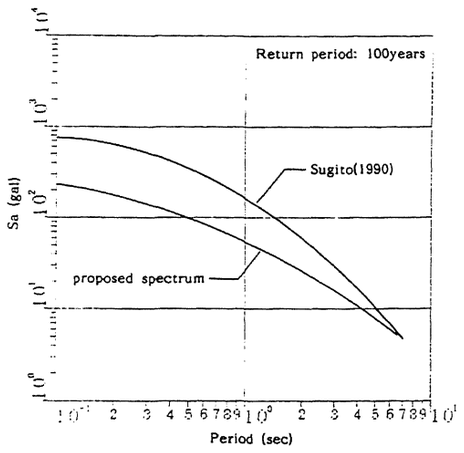

Figure 11. Estimated risk spectrum at the base rock level for Osaka City (return period: 100 years)

4 CONCLUSIONS

A risk map for the Kinki district was calculated by combining information from historical earthquake records and active fault data by the use of Bayes' theorem. The risk spectrum for the bed rock level was estimated from the proposed attenuation equation of the response spectrum. The procedure used and results obtained are

(1) Historical earthquake information and active fault data were combined by the use of Bayes' theorem. A seismic risk map for the Kinki district then was estimated from hazard curves at several hundreds of nodal points on a 20 x 20 km mesh of the Kinki area. The peak acceleration for the return period of 100 years is an expected 225 gal for Osaka City.

(2) We made a theoretical simulation of the response spectrum at the base rock level (v_s=3km) and established an attenuation equation for the maximum response acceleration for each natural period of that spectrum. A seismic risk analysis was made according to this attenuation law, and the risk spectrum calculated for Osaka City. If the amplification characteristics that exist between the base rock and upper layers can be determined, we can easily approximate the risk spectrum at a given layer.

ACKNOWLEDGEMENTS

We thank Profesor Kenzo Toki for his usuful suggestion and discussion on our study. We also greatfully acknowledge the contribution of our co-worker Kazuya Fujimura.

REFFERENCES

Alfredo H-S. Ang and Wilson H. Tang 1975. Probabilistic concepts in engineering planning and design. New York: John Wiley and Sons.

Cornell, C.A. 1968. Engineering seismic risk analysis. Bull. Seism. Soc. Am.:1583-1606.

Ejiri, J. and Y. Goto 1990. Data base of seismic information and waves. Technical Report, Obayashi Co.,Ltd. (in Japanese).

Ejiri, J. and Y. Goto: Characteristics of seismic ground motion at base rock level -- peak acceleration. Proc. of the 45th Annual Conference of the Japan Society of Civil Engineers 1: 1028-1029 (in Japanese).

Furuta, H. 1990. Research report on the safety and reliability estimation of bridges. Research group organized by the Kansai branch, JSCE: 176-186 (in Japanese).

Goto, H., M. Sugito, H. Kameda, H. Saito and T. Ootaki 1984. Prediction of nonstationary earthquake motions for moderate and great earthquakes on a rock surface. Annuals of Disas. Prev. Res. Inst., Kyoto Univ., No.27B-2: 30-50 (in Japanese with English abstract).

Irikura, K. 1983. Semi-empirical estimation of strong ground motion during large earthquake. Bull. Disas. Prev. Res. Inst., Kyoto Univ., Vol.33-2, No.298: 63-104.

Kameda, H. and T. Okumura 1985. Seismic hazard estimation based on active fault and historical earthquake data. Proc. of JSCE, Vol.362/I-4: 407-415 (in Japanese with English abstract).

Katayama, T. 1982. An engineering prediction model of acceleration response spectra and its application to seismic hazard mapping, Earthquake Engineering and Structural Dynamics, Vol.10: 149-163.

Kiureghian A. D. and A. H-S. Ang 1977. A fault-rupture model for seismic risk analysis. Bull. Seism. Soc. Am.: 1173-1194.

Midorikawa, S. and H. Kobayashi 1980. Isoseismal map in near-field with regard to fault rupture and site geological conditions. Trans. of A.I.J., No.290: 83-94.

Sato, T., J. Kiyono and T. Matuoka 1986. Attenuation of peak ground motion taking into account the fault extent. Proc. of 7th Japan Earthq. Eng. Symp.: 541-545.

Usami, T. 1975. Descriptive catalogue of disaster earthquakes in Japan. Tokyo: Univ. of Tokyo Press (in Japanese).

Utsu, T. 1979. Seismicity of Japan from 1885 through 1925: a new catalogue of earthquakes M<6 felt in Japan and smaller earthquakes which caused damage in Japan. Bull. Earthq. Res. Inst., Univ. of Tokyo, 54: 223-308 (in Japanese).

Wesnousky, S.G., C.H. Scholz, K.Shimazaki & T. Matsuda 1983. Earthquake frequency distribution and the mechanics of faulting. Jour. of Geophys. Res., Vol.88, No.B11: 9331-9340.